Research article

Electronic structures of lanthanum, samarium, and gadolinium sulfides

Lu Wang [1,¥], Chris M. Marin [2], Wai-Ning Mei [1,3], and Chin Li Cheung [2,3,*]

[1] Department of Physics, University of Nebraska at Omaha, Omaha, NE 68182, U.S.A.

[2] Department of Chemistry, University of Nebraska-Lincoln, Lincoln, NE 68588, U.S.A.

[3] Nebraska Center for Materials and Nanoscience, Lincoln, NE 68588, U.S.A.

[¥] Current address: Department of Materials Science and Engineering, University of Science and Technology of China, Hefei, Anhui 230026, China.

* Correspondence: Email: ccheung2@unl.edu; Tel: +1-402-472-5172; Fax: +1-402-472-9402.

Abstract: In this study, we report our efforts to elucidate the electronic structures of two lattice structures of lanthanide sulfides (LnS and Ln_3S_4) and for three lanthanides (Ln = La, Sm and Gd) using density functional theory calculations performed with the CASTEP code. A DFT+U method was used for the corrections of on-site Coulomb interactions with U = 6 eV. The calculated electronic structures show that both lanthanum and gadolinium sulfides have metallic properties, consistent with the available experimental results. However, the calculated electronic structure of Sm_3S_4 is considerably different from those of the La_3S_4 and Gd_3S_4 and is predicted to have semiconducting properties.

1. Introduction

Chalcogenide based semiconductors are a broad class of materials which display a wide variety of useful electronic properties. For example, copper indium gallium selenides and cadmium

tellurides are widely used in photovoltaics for power generation, [1] and bismuth tellurides are widely used for thermoelectric devices [2]. Additionally, while not as common as III-V semiconductor lasers such as gallium arsenide, zinc selenides have been used for lasing applications [3]. Moreover, cadmium tellurides, selenides, and sulfides are widely used for tunable fluorescent dyes (quantum dots) for medical research and diagnostics [4].

In the interest of extending the library of chalcogenide materials available for electronic applications, we have investigated the band structure and the partial density of states for three lanthanide sulfide systems. The lanthanide sulfides (Ln_xS_y) are a class of chalcogenides composed of a lanthanide cation (^{57}La–^{71}Lu) and the anion sulfur. Sulfur is, by convention, considered as the simplest chalcogen anion due to its similarities with selenium and tellurium and dissimilarity with oxygen. Although lanthanide cations tend to prefer to take a 3+ oxidation state, several lanthanides are known to additionally take a 2+ oxidation state, for instance, as in monosulfide (LnS) or mixed valence (Ln_3S_4) structures. Generally, La through Sm can most easily take the Ln_3S_4 mixed valence structure, while Gd through Dy are capable of taking this structure with S and Se, but not with Te [5]. It is important to note that although the Ln_3S_4 structure is nominally mixed valency, each Ln atom is crystallographically equivalent in this structure. More exotic is the lanthanide monosulfide (LnS) structure, in which the rare earth cations are entirely in the 2+ state. Of the lanthanide monosulfides, samarium monosulfide (SmS) has received by far the most attention. SmS was discovered as far back as 1956 [6], and is notable for the presence of a semiconducting low pressure phase and a metallic high pressure phase [7]. More recently, lanthanum monosulfide (LaS) has received increased attention due to its metallic properties and low work function, potentially making it suitable for use as a cold cathode material [8]. However, difficulty in preparing high quality lanthanide sulfide samples with controlled stoichiometry and high crystallinity have limited the understanding and electronic applications of this class of chalcogenides. Consequently, several authors have recommended using high quality band structure calculations to enable a better understanding of the electronic structures of lanthanide sulfides [9].

In order to rectify the lack of high quality data on the lanthanide sulfides, we have applied density functional theory (DFT) to predict the electronic structures of two specific crystal systems with varying sulfide content: the LnS structure and the Ln_3S_4 structure. Additionally, calculations with the lanthanide sulfides are very time-consuming to calculate, because of the need to take into account the effect of the *f*-shell electrons in these many atom unit cells. Thus, we have limited our study to three lanthanide group elements: lanthanum, samarium, and gadolinium.

2. Materials and Method

We applied density functional theory implemented in the CASTEP code [10] to calculate the band diagram and density of states of two lattice structures of lanthanide sulfides (LnS and Ln_3S_4) for three lanthanides (Ln = La, Sm and Gd). Spin-polarization was considered in the computation

because both Sm and Gd have unpaired spins in these structures. The unit cell of ideal LnS adopts the NaCl structure with space group Fm-3m (#225) symmetry. The lattice parameters for LaS, SmS and GdS were obtained from the International Centre for Diffraction Data (ICDD) and are a = 5.854 Å, a = 5.970 Å, and a = 5.562 Å, respectively. The unit cell of ideal Ln_3S_4 adopts the cubic symmetry with space group I-43d (#220). The lattice parameters for Ln_3S_4 were also obtained from the ICDD, and are: La_3S_4 (a = 8.73 Å), Sm_3S_4 (a = 8.556 Å), and Gd_3S_4 (a = 8.378 Å). Both crystal structures are illustrated in Figure 1. The LnS structure is a simple rock salt cubic structure. The Ln_3S_4 structure is considerably more complex, while still remaining cubic. This structure, prototyped by Th_3P_4, is a non-centrosymmetric body centered cubic system with the space group I-43d. In this structure, there are 18 lanthanide cations in each unit cell, with two located in each face along a diagonal glide plane, and the remaining 6 making up a distorted octahedron contained within the unit cell [11]. In spite of its complex appearance, the entire structure is composed of a single unique cation Wyckoff site and a single unique anion site.
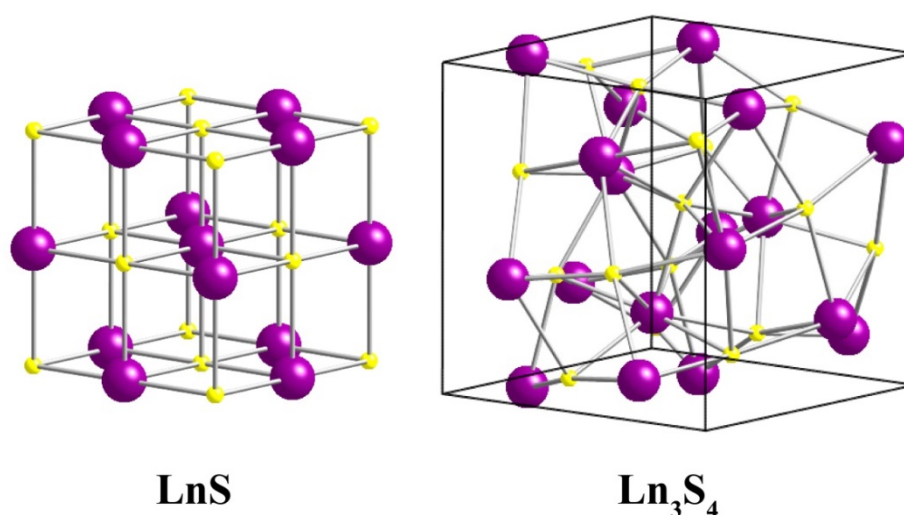

Figure 1. Unit cells of two lanthanide sulfides: (left) LnS and (right) Ln_3S_4 (Ln = La, Sm and Gd).

The plane wave basis set was utilized together with the generalized gradient approximation (GGA), and Perdew-Burke-Ernzerhof (PBE) exchange and correlation functional [12]. An energy cutoff of 380 eV was applied to the planewave basis set and ultra-soft pseudopotentials were employed with the valence electron configurations as $5s^25p^65d^16s^2$, $4f^75s^25p^65d^16s^2$, and $4f^65s^25p^66s^2$ for La, Gd, and Sm atoms, respectively. Brillouin zone integrations were performed with a Monkhorst-pack of $7 \times 7 \times 7$ k points for the LnS structures, while $5 \times 5 \times 5$ k points were used for the Ln_3S_4 structures. A Gaussian broadening was applied with a smearing width of 0.1 eV. The DFT+U method was used for the corrections of on-site coulomb interactions with U = 6 eV [13,14]

for the *f*-electrons of Sm and Gd. Moreover, the ensemble density functional theory (EDFT) [15,16] scheme programmed in CASTEP was used to overcome the convergence problem inherent in *f*-electron systems.

3. Results and Discussions

As the simplest lanthanide element, lanthanum serves as a natural place to start the discussion of the lanthanide sulfides, even though the electronic structure of LaS does exist in the literature [17]. Lanthanum takes a unique spot in the lanthanide series because it contains no f-shell electrons in its electronic structure of $[Xe]5d^16s^2$ [18], which greatly simplifies the electronic structure calculations for lanthanide sulfides. Additionally, the electronic structure of La_3S_4 generated considerable interest in the past due to its conducting to superconducting transition temperature at 7.2 K [19]. As shown in Figure 2, both LaS and La_3S_4 are expected to behave as a metal due to occupied bands overlapping the Fermi level (shown as 0 eV in our figures). More specifically, LaS is predicted to be a semimetal due to lower occupancy at the Fermi level with large density of states above and below. This indeed is consistent with the experimentally determined properties of LaS [8,20] and with previous calculations which made use of a full-potential linear muffin-tin orbital (LMTO) method for computing the band structure [17]. Similarly, La_3S_4 is predicted to be a metal. Although again there is a gap in energy bands less than 1 eV below the Fermi level, the calculated band structure of La_3S_4 has a high occupancy of *d*-orbitals at the Fermi level visible in the partial density of states (pDOS) (Figure 2). This is consistent with previously published experimental and computation results [19].

Samarium is typically believed to take the electronic structure $[Xe]4f^66s^2$ [18]. Unlike LaS, SmS is reported to be a narrow band gap semiconductor at atmospheric pressure and ambient temperature, but with a unique ability to switch to a metallic state at a moderately low pressure of 6.5 kbar [7]. Just as in the case of LaS, older LMTO methods were applied to simulate the band structure of SmS [21]. Our results, as shown in Figure 3, indicate SmS to be a narrow indirect band gap semiconductor with a gap of about 1 eV. This result corroborates with the observed semiconductor behavior of SmS, although it does differ from the experimental band gap of 0.15 eV [7]. Still, our calculation is an improvement from previous simulation results. Earlier work using a LMTO method predicted metallic behavior for SmS, and was forced to change the unit cell to 1.05 times the experimental values in order to introduce semiconductor behavior [21]. However, we have no reasons to doubt previous findings that a decrease in unit cell parameters (such as from high pressure) would force a narrowing of the band gap and reintroduce metallic character to the system.
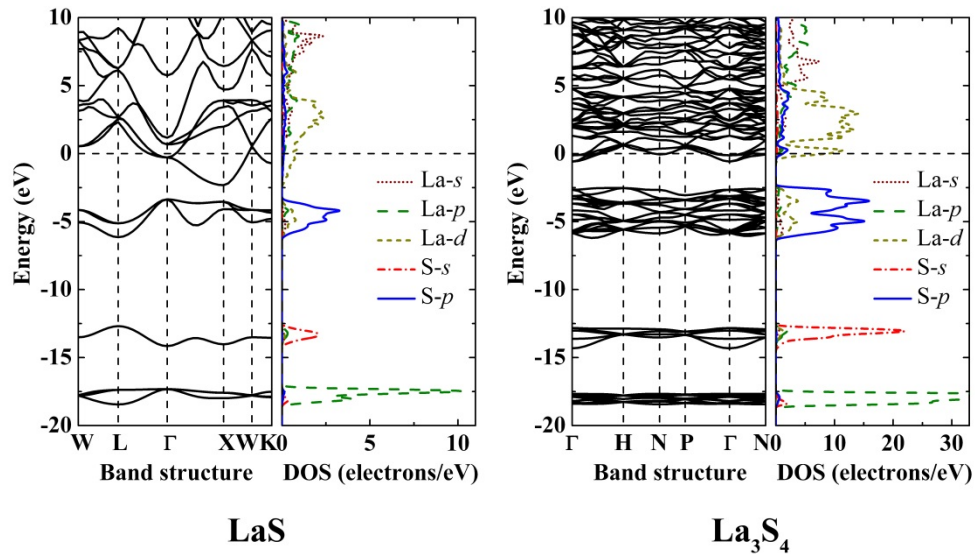
Figure 2. Band diagram and density of states of lanthanum sulfides: (left) LaS and (right) La$_3$S$_4$. The Fermi level is indicated by the dashed lines.

The electronic structure for Sm$_3$S$_4$, as shown in Figure 3, is in many ways the most surprising result of our calculations. Unlike the other systems, Sm$_3$S$_4$ has a large 2.1 eV band gap above the Fermi level. However, unlike in a well-behaved semiconductor, the Fermi level is not located inside the band gap. Instead, the Fermi level is 0.6 eV below the edge of the bottom bands, suggesting that technically Sm$_3$S$_4$ is a metal, but the large band gap's presence gives Sm$_3$S$_4$ character similar to that of an extremely degenerate semiconductor. Surprisingly, this result is consistent with the observed properties of experimental Sm$_3$S$_4$ samples. It was found that Sm$_3$S$_4$'s extinction coefficient trails off rapidly for photon energies below 2 eV (similar to a semiconductor with a 2 eV band gap) but remains appreciable all the way down to 0 eV (similar to a metal) [22]. Additionally, this is similar to the behavior of other samarium sulfides such as alpha phase Sm$_2$S$_3$ [23].
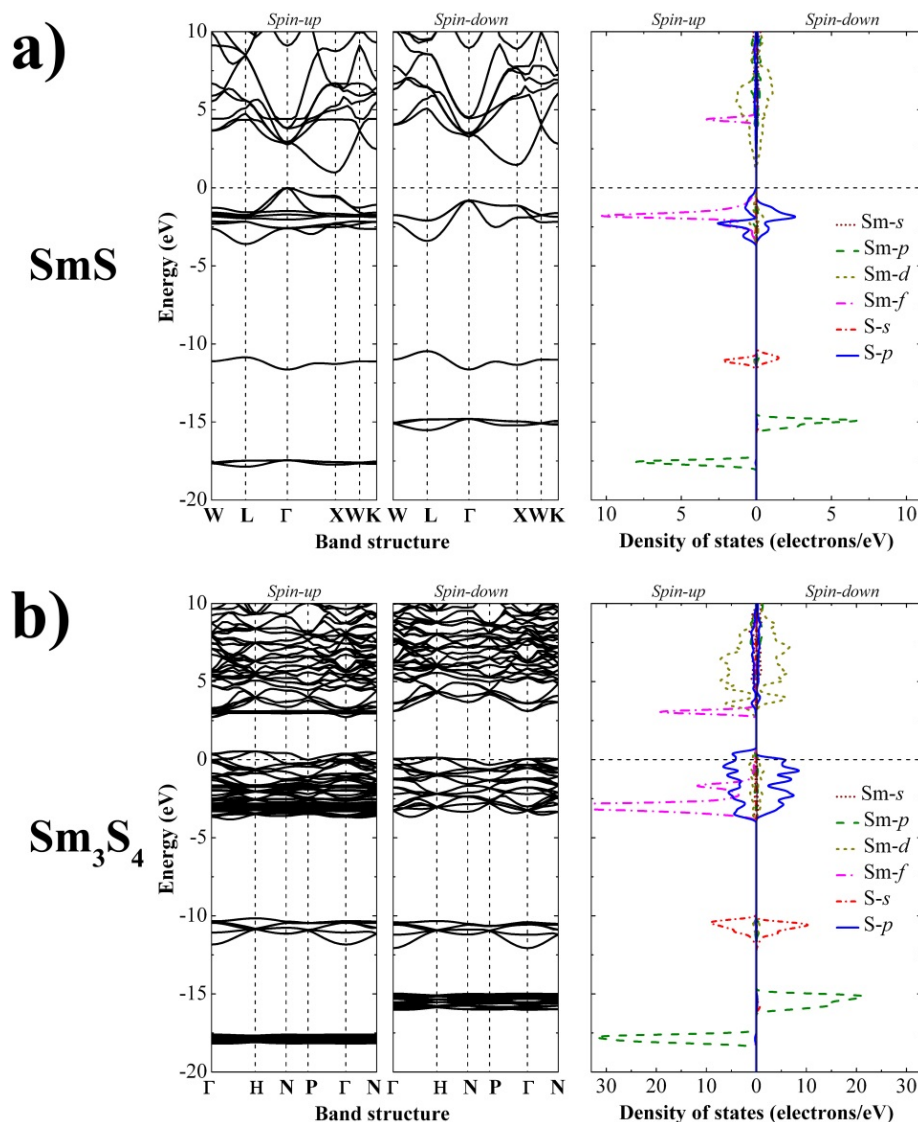
Figure 3. Band diagram and density of states of samarium sulfides: (a) SmS and (b) Sm₃S₄. The Fermi level is indicated by the dashed lines.

Unlike the simple case for lanthanum, gadolinium is expected to take the electronic structure of $[Xe]4f^7 5d^1 6s^2$ [18]. However, similar to LaS, our calculation predicted gadolinium monosulfide (GdS) to be a semimetal with occupied *d*-orbitals present at the Fermi level (Figure 4).

Additionally, just as in the case of La₃S₄, Gd₃S₄ is a semimetal with a wide gap in energy states extending from less than 1 eV below the Fermi level to several eVs below. The partial density of states for the gadolinium sulfides provides some clues for this similarity in electronic structure with those of the lanthanide sulfides: their occupied *f*-orbitals are at considerably lower energy levels than in the case of samarium (~ -12 eV for both gadolinium sulfides). This is likely a consequence of Gd containing a completely half-filled *f*-shell, which lowers the energy levels of these orbitals. These

results are in excellent agreement with the theoretical band structure of GdS and Gd_3S_4 conjectured from electron energy loss and photoemission spectroscopy experiments [24].
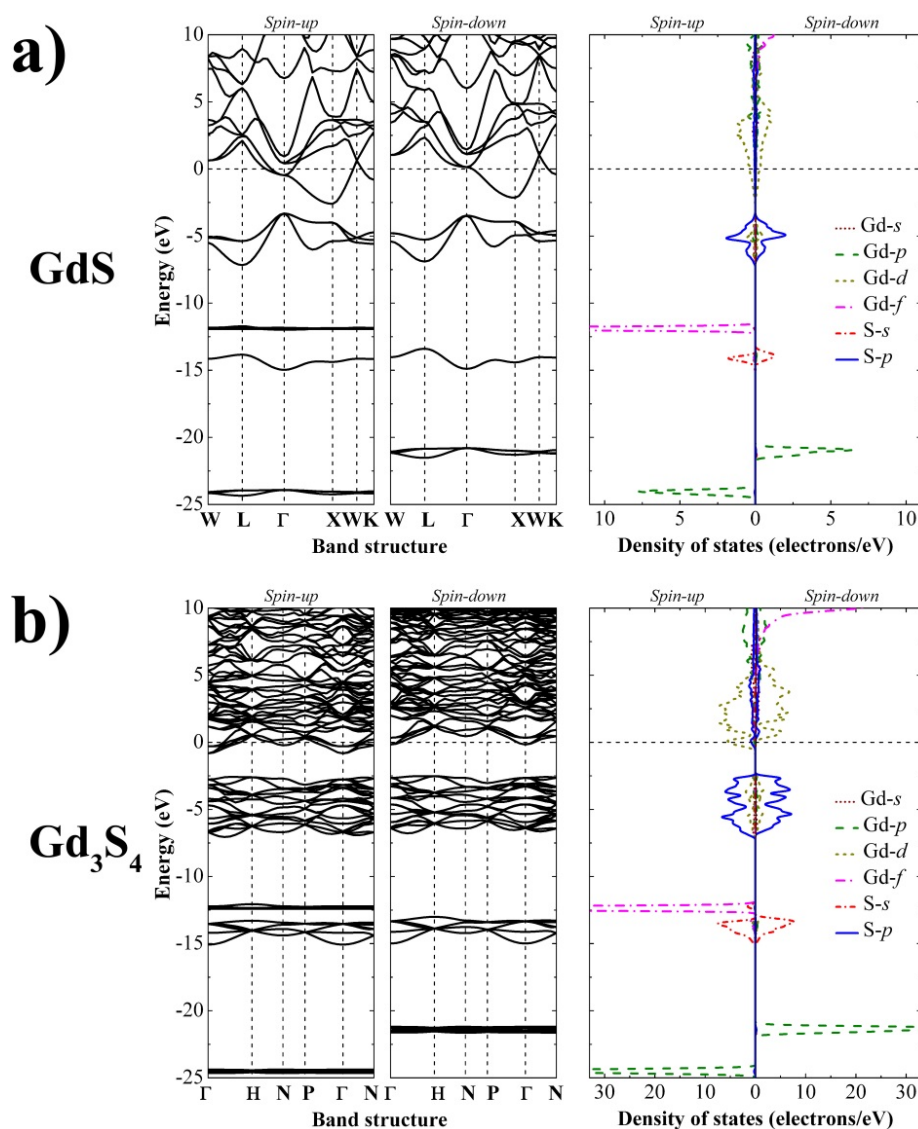

Figure 4. Band diagrams and density of states of gadolinium sulfides: (a) GdS and (b) Gd_3S_4. The Fermi level is indicated by the dashed lines.

4. Conclusion

Band structures and partial density of states have been calculated for LaS, La_3S_4, SmS, Sm_3S_4, GdS, and Gd_3S_4 using a DFT+U approach. To the best of our knowledge, this is the first time that this approach has been applied to most of these studied systems. Additionally, our calculation results have good correlation with existing experimental measurements for these systems. LaS, La_3S_4, GdS, and Gd_3S_4 are predicted to be semimetals. While SmS is predicted to be an indirect gap

semiconductor, Sm_3S_4 is expected to behave similarly to a heavily degenerate semiconductor. To improve the predictions of our computation method for other lanthanide systems where reliable *f*-orbital electronic contributions must be considered, further experimental measurement are needed to obtain a better estimation of the correction factor, U, for the on-site coulomb interactions.

Acknowledgements

Conflict of Interests

The authors report no conflict of interests in this research.

References

1. Parida B, Iniyan S, Goic R (2011) A review of solar photovoltaic technologies. *Renew Sust Energy Rev* 15: 1625–1636.
2. Dughaish ZH (2002) Lead telluride as a thermoelectric material for thermoelectric power generation. *Physica B* 322: 205–223.
3. Jeon H, Ding J, Patterson W, et al. (1991) Blue-green injection laser diodes in (Zn, Cd)Se/ZnSe quantum wells. *Appl Phys Lett* 59: 3619–3621.
4. Hardman R (2006) A toxicologic review of quantum dots: Toxicity depends on physicochemical and environmental factors. *Environ Health Perspect* 114: 165–172.
5. Gschneidner KA, Beaudry BJ (1995) Rare Earth Compounds, In: Rowe DM, *CRC Handbook for Thermoelectrics*, CRC Press.
6. Meyer G, Morss LR (1991) *Synthesis of lanthanide and actinide compounds*, Norwell: Kluwer Academic Publishers.
7. Batlogg B, Kaldis E, Schlegel A, et al. (1976) Electronic structure of Sm monochalcogenides. *Phys Rev B* 14: 5503–5514.
8. Fairchild S, Cahay M, Murray PT, et al. (2012) Grain size, texture, and crystallinity in lanthanum monosulfide thin films grown by pulsed laser deposition. *Thin Solid Films* 524: 166–172.
9. Witz C, Huhuenin D, Lafait J, et al. (1996) Comparative optical studies of Ce_2S_3 and Gd_2S_3 compounds. *J Appl Phys* 79: 2038–2042.
10. Segall MD, Philip JDL, Probert MJ, et al. (2002) First-principles simulation: ideas, illustrations and the CASTEP code. *Phys Condens Matter* 14: 2717–2744.

11. Holtzberg F, Methfessel S (1966) Rare-Earth Compounds with the Th_3P_4-Type Structure. *J Appl Phys* 37: 1433–1435.

12. Perdew JP, Burke K, Ernzerhof M (1996) Generalized gradient approximation made simple. *Phys Rev Lett* 77: 3865–3868.

13. Petersen M, Hafner J, Marsman M (2006) Structural, electronic and magnetic properties of Gd investigated by DFT+U methods: bulk, clean and H-covered (0001) surfaces. *J Phy—Condens Mat* 18: 7021–7043.

14. Jeffries JR, Veiga LSI, Fabbris G, et al. (2014) Robust ferromagnetism in the compressed permanent magnet Sm_2Co_{17}. *Physical Review B* 90.

15. Marzari N, Vanderbilt D, Payne MC (1997) Ensemble density functional theory for ab initio molecular dynamics of metals and finite-temperature insulators. *Phys Rev Lett* 79: 1337–1340.

16. Payne MC, Teter MP, Allan DC, et al. (1992) Iterative minimization techniques for ab initio total-energy calculations: Molecular dynamics and conjugate gradients. *Rev Mod Phys* 64: 1045–1097.

17. Eriksson O, Wills J, Mumford P, et al. (1998) Electronic structure of the LaS surface and LaS/CdS interface. *Phys Rev B* 57: 4067–4072.

18. Cotton FA, Wilkinson G (1966) *Advanced inorganic chemistry*; second ed.; Interscience Publishers: New York.

19. Shim JH, Kim K, Min BI, et al. (2002) Electronic structures of La_3S_4 and Ce_3S_4. *Physica B* 328: 148–150.

20. Cahay M, Boolchand P, Fairchild SB, et al. (2011) Review article: Rare-earth monosulfides as durable and efficient cold cathodes. *J Vac Sci Technol B* 29: 602–1–14.

21. Strange P (1985) A band theory description of the valence transition in samarium sulphide. *Physica* 130B: 44–46.

22. Batlogg B, Kaldis E, Schlegel A, et al. (1976) Optical and electrical properties of the mixed valence compound Sm_3S_4. *Solid State Commun* 19: 673–676.

23. Marin CM, Wang L, Brewer JR, et al. (2013) Crystalline α-Sm_2S_3 nanowires: Structure and optical properties of an unusual intrinsically degenerate semiconductor. *J Alloys Compd* 563: 293–299.

24. Grazhulis VA, Bozhko SI, Bolotin IL, et al. (1996) Electronic structure of the valence band of GdS_x and Gd_3S_4. *Appl Surf Sci* 104/105: 68–72.